EuroIntervention 2018;13:e2201-e2209 published online jaa November 2017 ■ published online e-edition April 2018

First serial optical coherence tomography assessment at baseline, 12 and 24 months in STEMI patients treated with the second-generation Absorb bioresorbable vascular scaffold

Janusz Kochman[1], MD, PhD; Łukasz Kołtowski[1]*, MD, PhD, FESC; Mariusz Tomaniak[1], MD; Jacek Jąkała[2], MD, PhD; Klaudia Proniewska[2], MSc, PhD; Jacek Legutko[3], MD, PhD; Tomasz Roleder[2], MD, PhD; Arkadiusz Pietrasik[1], MD, PhD; Adam Rdzanek[1], MD, PhD; Wacław Kochman[4], MD, PhD; Salvatore Brugaletta[5], MD, PhD; Grzegorz Opolski[1], MD, PhD, FESC; Evelyn Regar[6], MD, PhD, FESC

1. 1st Department of Cardiology, Medical University of Warsaw, Warsaw, Poland; 2. Krakow Cardiovascular Research Institute, Krakow, Poland; 3. Institute of Cardiology, Jagiellonian University Medical College, Krakow, Poland; 4. Faculty of Health Sciences, Medical University of Gdansk, Gdansk, Poland; 5. Institut Clinic Cardiovascular, IDIBAPS, Hospital Clinic, University of Barcelona, Barcelona, Spain; 6. University Heart Center, University Hospital Zürich, Zürich, Switzerland

J. Kochman and Ł. Kołtowski contributed equally to the manuscript as first authors.

This paper also includes supplementary data published online at: http://www.pcronline.com/eurointervention/133rd_issue/362

KEYWORDS

- bioresorbable scaffolds
- optical coherence tomography
- QCA
- STEMI

Abstract

Aims: The aim of the study was to assess the vascular healing response after Absorb bioresorbable vascular scaffold (BVS) implantation in patients with ST-segment elevation myocardial infarction (STEMI) utilising truly serial optical coherence tomography (OCT) examination at baseline, 12 and 24 months.

Methods and results: This was a single-centre, prospective, longitudinal study with baseline, 12- and 24-month OCT evaluation of 18 STEMI patients treated with 22 Absorb BVS. The healing pattern was evaluated based upon lumen area, neointimal hyperplasia, strut coverage and apposition. The lumen area decreased at 12 months compared to baseline (8.52±1.69 mm² vs. 7.0±1.70 mm², p<0.01), but it did not change from that point onwards up to 24 months (7.0±1.70 mm² vs. 6.94±1.65 mm², p=0.92). At 12 months after the index procedure, the mean neointimal thickness was 217±69 µm and further neointimal hyperplasia was observed between 12 and 24 months though less pronounced (Δ62±44 µm, p<0.0001). Full circumferential coverage of the vessel wall by neointima was observed in 92% of frames at 24 months. The low number of malapposed struts at the index procedure (<5%) further decreased over the observation period and was found in only one patient at 12 and 24 months. The ratio of uncovered struts was low at both 12 and 24 months.

Conclusions: This serial OCT analysis of the second-generation everolimus-eluting BVS in a STEMI population confirmed a favourable healing pattern as expressed by moderate neointimal growth, preserved lumen area and no late acquired malapposition.

**Corresponding author: 1st Department of Cardiology, Medical University of Warsaw, ul. Banacha 1a, PL-02-097 Warsaw, Poland. E-mail: lukasz@koltowski.com*

SUBMITTED ON 12/04/2017 - REVISION RECEIVED ON 1st 23/08/2017 / 2nd 02/11/2017 - ACCEPTED ON 13/11/2017

DOI: 10.4244/EIJ-D-17-00311

Abbreviations

ACS	acute coronary syndromes
ARC	Academic Research Consortium
BVS	bioresorbable vascular scaffold
CAD	coronary artery disease
DES	drug-eluting stents
HS	healing score
IQR	interquartile range
ISA	incomplete strut apposition
KCRI	Krakow Cardiovascular Research Institute
LA	luminal area
MLD	minimum luminal diameter
OCT	optical coherence tomography
PDLLA	poly(D,L-lactide)
PLLA	poly-L-lactide
pPCI	primary percutaneous coronary intervention
QCA	quantitative coronary angiography
RVD	reference vessel diameter
SD	standard deviation
STEMI	ST-segment elevation myocardial infarction
TIMI	Thrombolysis In Myocardial Infarction
TLR	target lesion revascularisation
%DS	percent diameter stenosis

Introduction

The bioresorbable vascular scaffold (BVS) has recently emerged as a new technology for the invasive treatment of coronary artery disease (CAD) that was designed to alleviate some of the drawbacks of metallic drug-eluting stents (DES). The possible advantages involve restoration of native vessel vasomotion, late lumen enlargement, plaque stabilisation and favourable remodelling. These effects have been confirmed in stable CAD patients using various imaging modalities with up to five years of follow-up[1-3]. Although some preliminary data on the safety and feasibility of BVS implantation in patients with acute coronary syndromes (ACS) are available[4-6], observations on their long-term performance are lacking[7].

The different underlying pathophysiology of ST-segment elevation myocardial infarction (STEMI) involving a ruptured thrombotic plaque, presence of necrotic core, vasoconstriction, and overall enhanced pro-coagulant status might negatively impact on vessel healing. This has been demonstrated in studies with metallic stent implantation, where the large necrotic burden impaired the strut endothelialisation. Therefore, optical coherence tomography (OCT), which allows detailed intravascular assessment, may potentially bring valuable insights into the long-term healing response after BVS implantation in this patient subset. So far, OCT has not been used in a truly serial fashion in a STEMI population. Given this background, we present the first serial, long-term OCT observation after BVS implantation in patients with STEMI.

Materials and methods

POPULATION, DEVICE AND STUDY DESIGN

The study population and design of this single-centre, prospective registry of STEMI patients who underwent primary percutaneous coronary intervention (pPCI) with Absorb™ BVS (Abbott Vascular, Santa Clara, CA, USA) implantation has already been described[7].

In this present analysis we report clinical, angiographic and OCT outcomes of 18 STEMI patients (22 scaffolds) in whom the data were obtained at baseline, 12- and 24-month follow-up. The study flow chart is presented in **Supplementary Figure 1**. Informed consent was obtained from all patients and the local ethics committee approved the study protocol.

All enrolled patients were older than 18 years, had chest pain for up to 12 hours, met the ECG criteria for STEMI according to the European Society of Cardiology guidelines[8] and had *de novo* native coronary artery lesions suitable for treatment with Absorb BVS 2.5, 3.0 or 3.5 mm in diameter and 18 or 28 mm in length. Detailed characteristics of the implanted device have been described previously[9]. The clinical characteristics of the screened patient population are provided in **Supplementary Table 1**.

PCI procedures were performed according to routine interventional techniques. Predilatation was recommended by the study protocol. OCT was scheduled once an optimal angiographic result was achieved.

In patients in whom OCT showed evidence of incomplete strut apposition (ISA) of more than 350 µm, post-dilatation was recommended. The threshold of 350 µm was set based on the results from DES trials that reported a tenfold higher rate of persistent ISA in stents with intermediate (300-500 µm) as compared to moderate (100-300 µm) malapposition distance at baseline[10]. In case of major dissection or scaffold underexpansion on OCT, further intervention (e.g., post-dilatation and additional scaffold implantation) was allowed. Dual antiplatelet therapy was mandatory for 12 months after pPCI.

Patients were scheduled for serial angiographic and OCT evaluation at 12-month intervals. Scaffold thrombosis and recurrent MI were defined according to the Academic Research Consortium (ARC) definitions[11].

CORONARY ANGIOGRAPHY AND OCT ANALYSES

Detailed methodology of clinical, angiographic, and OCT assessment has been described previously[7]. Off-line qualitative and quantitative coronary angiography (QCA) was analysed using the Cardiovascular Angiography Analysis System 5.11.1 (Pie Medical Imaging Systems, Maastricht, the Netherlands)[1,12]. Late lumen loss was calculated as the difference between the post-procedural, 12- and 24-month minimum luminal diameter (MLD) **(Figure 1)**.

OCT images were acquired with a commercially available frequency domain OCT imaging system (C7-XR™ system with Dragonfly™ image catheters; LightLab Imaging/St. Jude Medical, Inc., Westford, MA, USA) and analysed by an independent core laboratory (Krakow Cardiovascular Research Institute [KCRI], Krakow, Poland) by analysts blinded to the angiographic data and clinical characteristics, using proprietary LightLab off-line analytical software.

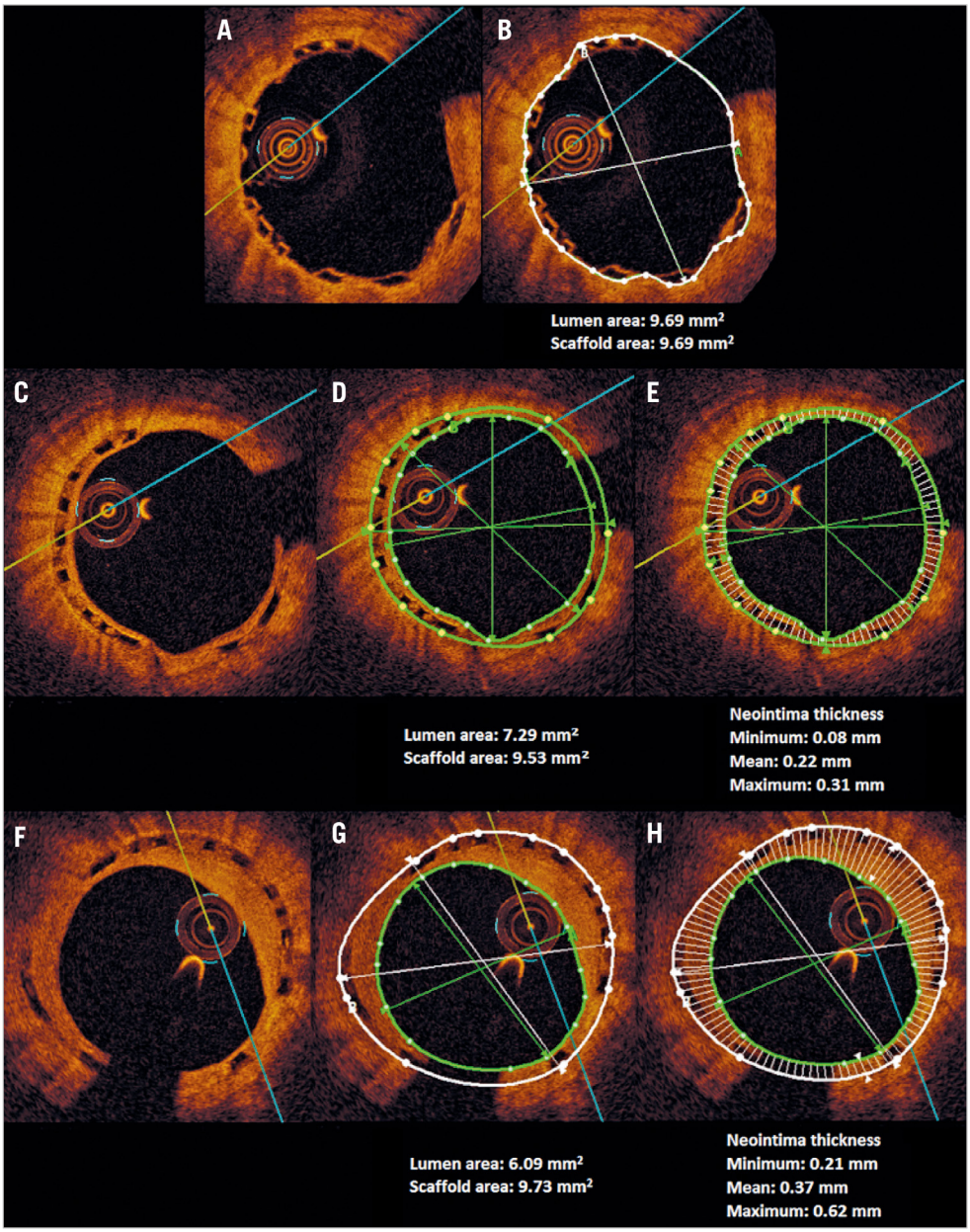

Figure 1. *Example of optical coherence tomography (OCT) image analysis. Corresponding frames of the cross-sectional view of the same scaffold after index post-procedure (A, B), at one-year follow-up (C, D, E) and two-year follow-up (F, G, H) are shown together with the measurements of lumen and scaffold area (B, D, G) and neointimal thickness as well as its distribution (E, H). The minimum, maximum and mean of neointimal thickness are presented.*

The methodology of OCT evaluation was based on previous studies using OCT assessment of BVS[6,13-16] and is presented in the **Supplementary Appendix**.

STATISTICAL ANALYSIS

Statistical analysis was performed using the JMP software, version 9.0.0 (SAS Institute, Cary, NC, USA). Continuous variables are presented as the mean±standard deviation (SD) (normal distribution) and as the median with interquartile range (IQR) (non-normal distribution), whereas categorical variables are presented as absolute values and percentages. The Wilcoxon signed-rank test was used for two related sample comparisons, and the Pearson correlation coefficient for continuous variables. Mixed models were used to take into account the clustered nature of OCT data regarding struts, malapposition, segments and edges. OCT intra- and inter-observer variability in the analysis of lumen area and scaffold area was assessed.

Results

Out of 23 patients initially included in the study, four subjects were not evaluated at the 12-month follow-up for reasons provided previously[7], while one patient withdrew consent for the 24-month OCT evaluation. The baseline characteristics of the remaining 18 patients

are presented in **Table 1** and **Supplementary Table 2**. Between 12 and 24 months there was no incidence of death, recurrent MI or scaffold thrombosis. One target lesion revascularisation (TLR) was identified 620 days after the index procedure due to focal in-scaffold restenosis treated with elective angioplasty with a drug-eluting stent.

QUANTITATIVE CORONARY ANGIOGRAPHY ANALYSIS

Serial QCA analysis revealed that MLD decreased from 2.65±0.41 mm to 2.49±0.46 mm and 2.10±0.46 mm at 12 and 24 months, respectively. The initial late lumen loss of 0.10±0.23 mm at 12 months increased to 0.49±0.38 mm at 24 months. This was associated with an increase in the intra-scaffold diameter stenosis from 10.84±9.75% to 15.85±11.2% at 12 months and 25.4±12.46% at 24 months **(Table 2)**.

OPTICAL COHERENCE TOMOGRAPHY ANALYSIS

At two years, there was a substantial decrease in the mean luminal area (LA), which was driven by its reduction during the first year. From 12 months onwards, the mean LA remained stable. The observed loss of LA was caused by a substantial neointimal growth during the first 12 months (217±69 μm), whereas in the second year it was still present, though less pronounced (Δ62±44 μm, $p<0.01$) **(Table 3, Supplementary Table 3, Figure 2)**. The detailed analysis of changes in mean LA of the proximal and distal adjacent peri-scaffold segments as well as in-scaffold segments categorised into proximal, central and distal parts at different time points is shown in **Supplementary Table 4** and **Supplementary Table 5**. In the first 12 months, there was a consistent decrease of the LA in all three in-scaffold segments. Over the second year, LA in the proximal and distal scaffold segments remained unchanged, whereas in the middle segment there was a trend towards LA increase.

The distribution of neointimal tissue was characterised by an increase of homogeneity at 24 months, compared to that observed after one year, as expressed by the greater symmetry index

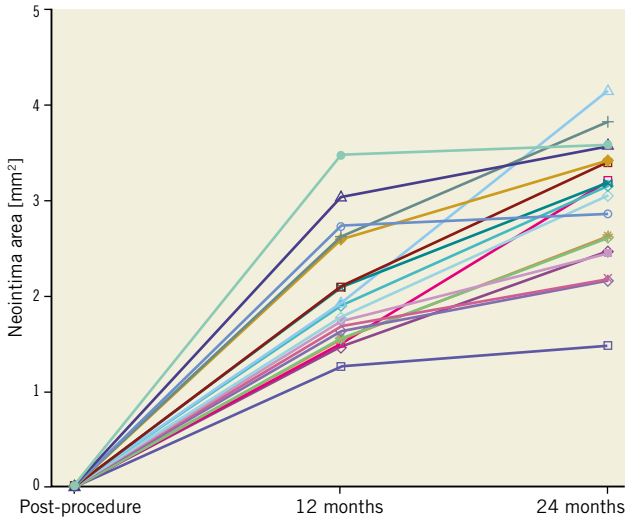

Figure 2. *Neointimal area changes over the 24 months of follow-up.*

Table 1. Baseline angiographic and procedural characteristics (n=18 patients)*.

Patient characteristics		n=18
Unfractionated heparin, n (%)		18 (100.0)
Use of GP IIb/IIIa inhibitors, n (%)		17 (94.4)
Transradial approach, n (%)		17 (94.4)
Door-to-balloon time (mean±SD, min)		31.3±19.8
Target vessel, n (%)	LAD	3 (16.7)
	Cx	3 (16.7)
	RCA	12 (66.6)
AHA/ACC lesion classification, n (%)*	A	0 (0.0)
	B1	2 (10.0)
	B2	11 (55.0)
	C	7 (35.0)
Diameter stenosis at baseline (mean±SD, %)		86.78±11.87
Maximal proximal reference diameter (mean±SD, mm)		3.23±0.72
Maximal distal reference diameter (mean±SD, mm)		2.92±0.67
Number of scaffolds per lesion, n (%)	1 scaffold	18 (90.0) lesions
	2 scaffolds	2 (10.0) lesions
Direct stenting, n (%)		4 (20.0)
Predilatation, n (%)		16 (80.0)
Post-dilatation, n (%)		14 (70.0)
Manual thrombectomy, n (%)		11 (61.1)
TIMI at baseline, n (%)	0	11 (61.0)
	1	1 (5.6)
	2	5 (27.8)
	3	1 (5.6)
TIMI at final, n (%)	2	1 (5.6)
	3	17 (94.4)
Thrombus grade at baseline, n (%)	0	4 (20.0)
	1	0 (0.0)
	2	1 (5.0)
	3	1 (5.0)
	4	3 (15.0)
	5	11 (55.0)
Nominal scaffold diameter (median, IQR, mm)		3.0 (3.0-3.5)
Nominal scaffold length (median, IQR, mm)		28 (18-36)
Nominal non-compliant balloon length (median, IQR, mm)		12 (12-15)
Nominal non-compliant balloon diameter (median, IQR, mm)		3.0 (3.0-3.5)

Data are expressed as mean±SD, median and IQR or number (n) and percentage (%). Angiographic thrombus grading at baseline: grade 0: no thrombus; grade 1: possible thrombus; grade 2: the thrombus' greatest dimension is <1/2 vessel diameter; grade 3: greatest dimension >1/2 to <2 vessel diameters; grade 4: greatest dimension >2 vessel diameters; grade 5: total vessel occlusion due to thrombus. *Data are presented for 18 patients, 20 lesions and 22 scaffolds as two patients received two scaffolds at different non-overlapping sites (second culprit lesion), and another two patients received overlapping scaffolds. AHA/ACC: American Heart Association/American College of Cardiology; Cx: left circumflex; IQR: interquartile range; LAD: left anterior descending; RCA: right coronary artery; SD: standard deviation

Table 2. Paired quantitative coronary angiography analysis (scaffold level, n=22).

Variable	Post procedure	12 months	24 months	Baseline –12 months *p*-value	12-24 months *p*-value	Baseline –24 months *p*-value
Reference vessel diameter (mm)	2.89±0.55	2.97±0.50	2.83±0.46	0.59	0.04	0.19
Minimal luminal diameter (mm)	2.65±0.41	2.49±0.46	2.10±0.46	0.10	<0.01	<0.01
Diameter stenosis (%)	10.9±9.75	15.9±11.20	25.4±12.46	0.08	<0.01	<0.01
Late lumen loss (mm)	–	0.10±0.23	0.49±0.38	–	<0.01	–
Data are expressed as mean±SD.						

(Table 3). Similarly, an improvement in neointimal tissue coverage was observed with an entire circumference covered in 92% of frames at 24 months.

The scaffold area expanded over the entire observation period, with the most significant increase between 12 and 24 months **(Table 3, Figure 3)**. Significant differences in the dynamic of the scaffold area changes between the in-scaffold segments were observed. It was numerically more pronounced in the middle segment (Δ1.16±0.42 μm) than in the proximal (Δ0.88±0.51 μm) and distal (Δ0.58±0.36 μm) in-scaffold segments over the second year **(Supplementary Table 4)**.

The total number of uncovered struts was very low at 24 months (<0.5%). Uncovered struts were observed in eight cases at 12 months and five cases at 24 months, with an average uncovered strut ratio of 2.5±2.0% and 1.7±2.1%, respectively **(Table 3)**.

After two years, malapposition was rare and found in only one patient (11 malapposed struts), in whom this phenomenon was already present at 12 months (16 malapposed struts) **(Figure 4)**. There were no malapposed uncovered struts observed in this cohort at 12 and 24 months. Also, the healing score (HS) favourably decreased between 12 and 24 months (2.33±4.6 vs. 1.09±2.77, p<0.0001) **(Table 3, Figure 5)**.

Table 3. Serial optical coherence tomography analysis (scaffold level, n=22).

Variable	Post procedure	12-month follow-up	24-month follow-up	Baseline –12 months	12-24 months	Baseline –24 months	Baseline –12 months *p*-value	12-24 months *p*-value	Baseline –24 months *p*-value
Minimum lumen area (mm^2)	6.64±1.40	4.95±1.70	4.60±1.53	–1.69±1.19	–0.35±0.96	–2.04±1.13	<0.01	0.11	<0.01
Minimum flow area (mm^2)	6.55±1.44	4.95±1.70	4.60±1.53	–1.69±1.23	–0.35±0.96	–2.08±1.15	<0.01	0.13	<0.01
Mean lumen area (mm^2)	8.52±1.69	7.00±1.70	6.94±1.65	–1.52±1.0	–0.06±0.85	–1.58±1.12	<0.01	0.92	<0.01
Mean flow area (mm^2)	8.42±1.69	7.00±1.70	6.94±1.65	–1.55±0.98	–0.06±0.85	–1.59±1.20	<0.01	0.73	<0.01
Minimum scaffold area (mm^2)	6.97±1.49	7.18±1.47	7.27±1.70	0.21±1.09	0.09±0.84	0.30±0.98	0.45	0.76	0.42
Mean scaffold area (mm^2)	8.33±1.56	8.99±1.50	9.84±1.74	0.66±0.90	0.85±0.86	1.51±1.22	0.01	<0.01	<0.01
Scaffold-to-vessel diameter ratio	1.00±0.00	1.15±0.08	1.20±0.07	0.15±0.08	0.05±0.04	0.20±0.07	<0.01	<0.01	<0.01
Scaffold area obstruction (%)	0.00±0.00	23±8.9	30.1±7.6	23±8.9	7.1±5.1	30.1±7.6	<0.01	<0.01	<0.01
Distal reference mean lumen area (mm^2)	6.92±3.39	7.00±2.90	6.79±2.71	–0.08±2.17	–0.21±1.06	–0.13±1.87	0.63	0.12	0.56
Proximal reference mean lumen area (mm^2)	8.71±3.19	8.35±3.06	8.38±2.99	–0.36±2.03	–0.03±1.06	–0.12±2.44	0.06	0.67	0.24
Malapposed strut ratio (%)	5.0±8.4	0.3±1.5	0.2±1.1	–3.6±7.1	–0.3±0.4	–4.8±7.5	0.01	0.33	0.01
Malapposed strut ratio (%) in patients with any malapposed strut	9.11±15.10	0.80±3.58	0.55±2.46	–8.31±12.21	–0.25±1.12	–8.56±13.07	<0.01	1.00	<0.01
Malapposition distance (mm)	0.12±0.09	0.03±0.12	0.02±0.09	–0.09±0.11	–0.01±0.03	–0.10±0.09	<0.01	0.33	0.01
Malapposition area (mm^2)	0.33±0.49	0.07±0.31	0.05±0.21	–0.26±0.38	–0.02±0.09	–0.28±0.39	<0.01	0.33	<0.01
Mean neointima thickness (μm)	0±0	217±69	279±55	217±69	62±44	279±55	<0.01	<0.01	<0.01
Maximum neointimal thickness (μm)	0±0	362±83	436±78	362±83	74±61	436±78	<0.01	<0.01	<0.01
Neointima area (mm^2)	0.00±0.00	1.99±0.60	2.90±0.67	1.99±0.60	0.91±0.52	2.90±0.67	<0.01	<0.01	<0.01
Symmetry of the neointima thickness	–	0.16±0.14	0.29±0.12	–	–0.13±0.10	–	–	<0.01	–
Uncovered strut ratio (%)	–	1.0±1.8	0.4±1.2	–	–0.6±2.2	–	–	0.24	–
Uncovered strut ratio (%) in patients with any uncovered struts	–	2.5±2.0	1.7±2.1	–	–0.8±5.0	–	–	1.00	–
Scaffolds with >0 uncovered struts, n (%)	–	8 (36.4)	5 (22.7)	–	3	–	–	0.91	–
Scaffolds with >0 malapposed struts, n (%)	14 (63.6)	1 (4.5)	1 (4.5)	13	0	13	<0.01	1.00	<0.01
Healing score	–	2.33±4.6	1.09±2.77	–	1.24±4.48	–	–	<0.0001	–
Data expressed as mean±SD or count and percentage (%).									

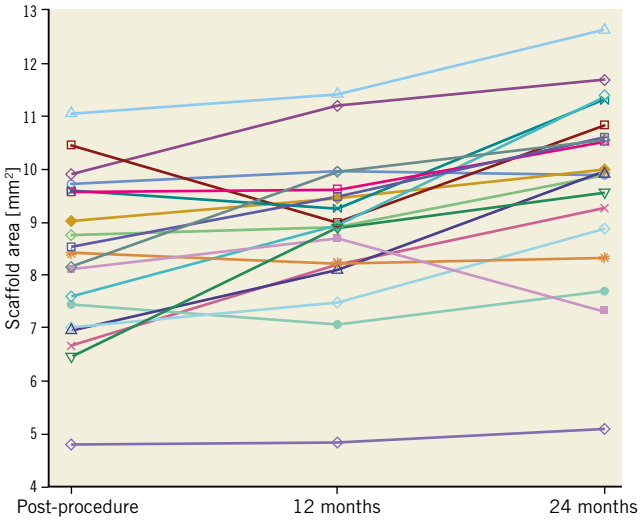

Figure 3. *Scaffold area changes between baseline, 12- and 24-month follow-up.*

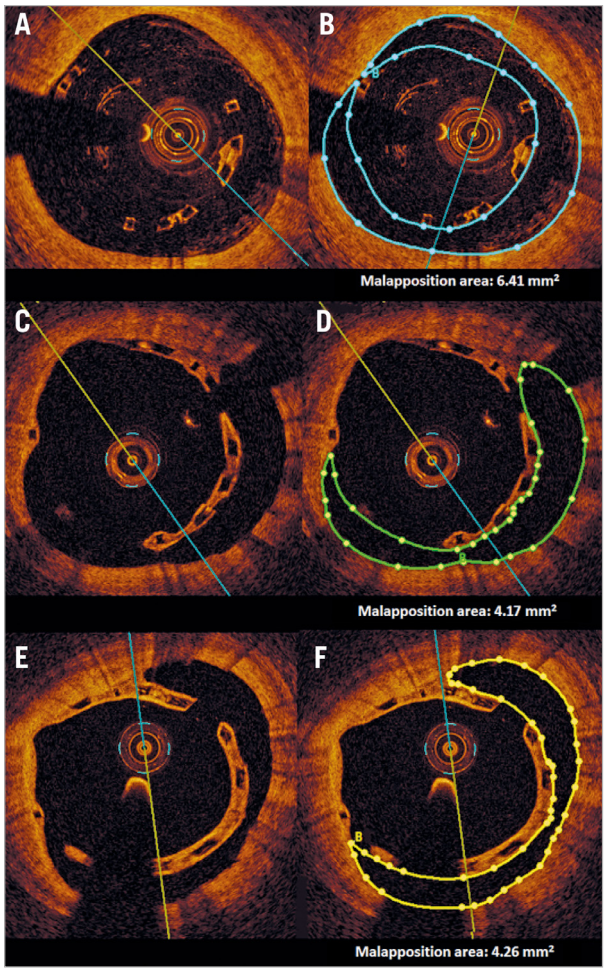

Figure 4. *The stages of malapposition at three time points, and the measurement methodology of the malapposition area. The first row presents post-procedure frames without (A) and with (B) delineation of malapposition area. Corresponding frames with persisting malapposition at 12 (C & D) and 24 months (E & F) are presented.*

Strut discontinuity was noted in three patients at 24 months. All cases occurred in the second year and none were detected at baseline and 12 months. The struts with discontinuity were covered, with no signs of malapposition. None of these patients experienced any major adverse cardiac events and all had discontinued dual antiplatelet therapy at 12 months.

The quality of the measurements was confirmed by a low inter- and intra-observer variability, calculated for lumen and scaffold area. For inter-observer variability, the mean relative difference was 0.17±4.75% for lumen area and 2.70±5.09% for scaffold area; for intra-observer variability, the mean relative difference was 0.37±1.13% for lumen area and 0.01±2.05% for scaffold area **(Supplementary Figure 2)**.

Discussion

Although limited preliminary clinical data on the safety and efficacy of BVS implantation in STEMI patients have already been published, detailed evaluation of the midterm healing response utilising high-resolution intravascular imaging is lacking. This is the first study to report truly serial angiographic and OCT assessment at baseline, 12- and 24-month follow-up. The findings could be summarised as follows. A) Over the first year a marked vascular reaction was observed, as expressed by i) a substantial neointimal proliferation, associated with ii) a significant decrease in lumen area, partially compensated by iii) an increase in scaffold area. B) Over the second year, a continuation of the healing process of the treated segment was noted with i) mild neointimal growth, ii) increase in scaffold area resulting in iii) sustained lumen area, and iv) no late acquired strut malapposition.

These favourable patterns of lumen preservation, scaffold expansion and mild neointima proliferation have been previously reported in a stable angina cohort treated with Absorb BVS implantation[3,16,17]. Although the midterm follow-up in these studies was performed at slightly different time points, there was a consistent deceleration of neointimal growth accompanied by increasing scaffold expansion. This may indicate consistent vessel healing response irrespective of the baseline clinical setting.

Interestingly, although the mean LA in OCT remained stable over the second year, the scaffold segment analysis revealed a trend towards an increase in the lumen area of the middle in-scaffold segment between 12 and 24 months. This was associated with a significant increase in the scaffold area, which dynamic was more pronounced in the middle in-scaffold segment than in the proximal and distal segments. These intriguing findings can potentially be explained by the intensive post-dilatation technique with non-compliant balloons used mainly within the middle part of the scaffold to avoid edge dissection.

The observed loss of device integrity is an anticipated sign of a programmed process of scaffold bioresorption, which in our cohort was further confirmed by the occurrence of strut discontinuities, found in three cases at 24 months. Although the strut stability might be challenged by both scaffold dissolution and device overstretch at baseline, the latter phenomenon is unlikely

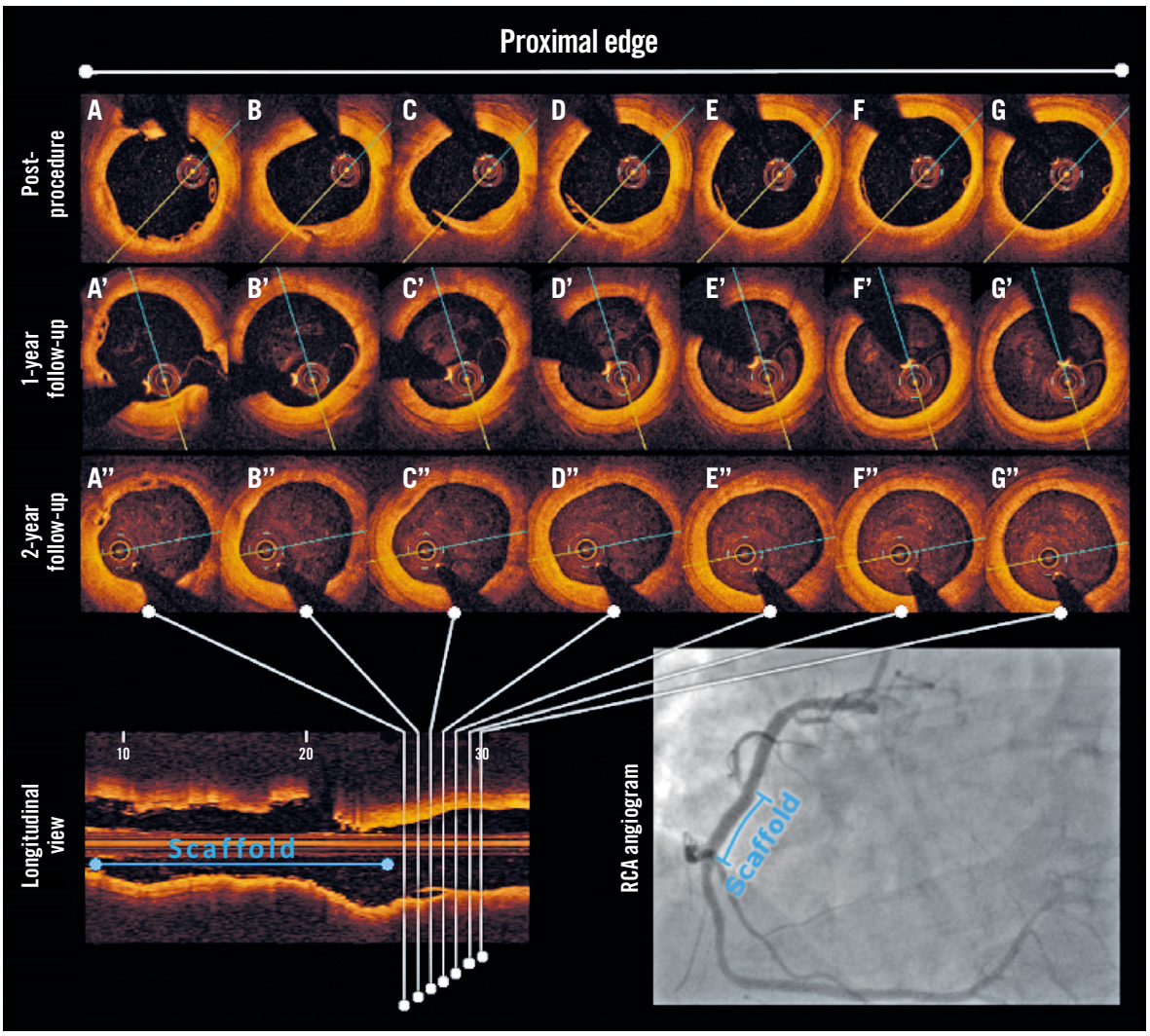

Figure 5. *Serial OCT evaluation of the healing process of a post-procedural edge dissection after BVS implantation. Dissection is visible at baseline (A-G), whereas at 12 (A'-G') and 24 months (A"-G") it was no longer detectable, indicating completion of the healing process.*

in our study as strut fractures were not observed at baseline or at 12 months. Disappearance of polymeric struts, previously reported at 24 months in nearly 30% of first-generation BVS, was not revealed in the present investigation. This is probably explained by the more controlled and longer duration of the resorption processes attributed to the second-generation BVS used in this study. Full bioresorption might be expected at four years with the contemporary version of the more slowly bioresorbing scaffolds. However, it should be taken into consideration that OCT imaging has not been validated as a tool to evaluate the degree of BVS degradation, and the appearance of black areas in place of struts is not confirmatory of struts remaining, rather a lack of recellularisation.

OCT revealed a mild increase of neointimal thickness and symmetry index over the second year. The "late catch-up phenomenon", understood as neointimal proliferation beyond six months, has been reported previously in BVS and DES[18,19]. Although in metallic stents it may lead to an unfavourable increase of late lumen loss, it seemed to be of limited concern in BVS due to the observed scaffold expansion resulting from the programmed bioresorption process, as reported in the first-in-man studies[1,3,13,16].

Our findings are in line with the recent data from the ABSORB II trial. This showed that late lumen loss was even larger in patients treated with BVS, compared with DES (0.37 mm vs. 0.25 mm; p=0.78 for non-inferiority) bringing into question the late lumen area one should be considering as, until complete scaffold resorption, the vessel wall is subject to biochemical interactions with the polymer that could lead to inflammatory response and subsequent neoatherosclerosis.

Although acute strut malapposition was seen in 14 out of 18 patients, the mean rate of strut malapposition was very low (<5%), and after 12 months a further numeric decrease in the number of malappossed struts, malapposition distance and area was observed. Of note, no late acquired malapposition was found. Similarly, Ormiston et al found signs of acute malapposition in a substantial number of patients, that decreased significantly after 24 months[16]. Also, the recent ABSORB Japan study confirmed a reduction in

malapposition rates and number of uncovered struts at two years, which was found to be comparable with that observed in DES[20].

Overall, between 12 and 24 months a favourable healing pattern was observed, as quantified by the decrease in the HS, that at 24 months reached substantially lower values, compared to previous studies with BVS in STEMI with shorter follow-up duration[6].

Study limitations

The results of this study have to be viewed in the light of the following limitations. First, the size of the analysed cohort is small. However, these are the first truly serial OCT data on the long-term OCT follow-up of BVS, hence the potential patient-to-patient variability was minimised. The second limitation is the non-randomised design of this study and the lack of a control group. Thirdly, no qualitative assessment of neointima was performed. Fourthly, a discrepancy between the imaging methods (QCA vs. OCT) has been observed; therefore, the final conclusion regarding changes in the lumen area should be interpreted with caution. However, these lumen measurements cannot be directly compared given the different nature of QCA and OCT methodologies. Taking into account that the spatial resolution of OCT is superior to coronary angiography allowing more precise evaluation of lumen eccentricity, the data obtained with this imaging modality might be perceived as more reliable. Therefore, we have based our reasoning and discussion on OCT measurements.

Conclusions

Overall, our observations indicate a favourable healing pattern after BVS implantation in STEMI patients at two years of OCT follow-up, with maintenance of lumen area, almost complete neointimal strut coverage and significant reduction of strut malapposition. However, due to the small number of patients, these data should be interpreted with caution and larger trials are needed to draw any firm conclusions.

Impact on daily practice

In the long term, bioresorbable vascular scaffolds in ST-segment elevation myocardial infarction have mainly been evaluated for clinical outcomes. The precision of intravascular imaging allows the detection of signals for potential adverse events with high sensitivity. The detailed results of this serial OCT imaging study provide reassurance on patient safety and may facilitate further usage of bioresorbable vascular scaffolds in ST-segment elevation myocardial infarction patients.

Conflict of interest statement

The authors have no conflicts of interest to declare.

References

1. Ormiston JA, Serruys PW, Regar E, Dudek D, Thuesen L, Webster MW, Onuma Y, Garcia-Garcia HM, McGreevy R, Veldhof S. A bioabsorbable everolimus-eluting coronary stent system for patients with single de-novo coronary artery lesions (ABSORB): a prospective open-label trial. *Lancet.* 2008;371:899-907.

2. Serruys PW, Onuma Y, Dudek D, Smits PC, Koolen J, Chevalier B, de Bruyne B, Thuesen L, McClean D, van Geuns RJ, Windecker S, Whitbourn R, Meredith I, Dorange C, Veldhof S, Hebert KM, Sudhir K, Garcia-Garcia HM, Ormiston JA. Evaluation of the second generation of a bioresorbable everolimus-eluting vascular scaffold for the treatment of de novo coronary artery stenosis: 12-month clinical and imaging outcomes. *J Am Coll Cardiol.* 2011;58:1578-88.

3. Karanasos A, Simsek C, Gnanadesigan M, van Ditzhuijzen NS, Freire R, Dijkstra J, Tu S, van Mieghem N, van Soest G, de Jaegere P, Serruys PW, Zijlstra F, van Geuns RJ, Regar E. OCT assessment of the long-term vascular healing response 5 years after everolimus-eluting bioresorbable vascular scaffold. *J Am Coll Cardiol.* 2014;64:2343-56.

4. Diletti R, Karanasos A, Muramatsu T, Nakatani S, van Mieghem NM, Onuma Y, Nauta ST, Ishibashi Y, Lenzen MJ, Ligthart J, Schultz C, Regar E, de Jaegere PP, Serruys PW, Zijlstra F, van Geuns RJ. Everolimus-eluting bioresorbable vascular scaffolds for treatment of patients presenting with ST-segment elevation myocardial infarction: BVS STEMI first study. *Eur Heart J.* 2014;35:777-86.

5. Rzeszutko Ł, Siudak Z, Włodarczak A, Lekston A, Depukat R, Ochała A, Gil RJ, Balak W, Marć M, Kochman J, Zasada W, Dudek D. Use of bioresorbable vascular scaffolds in patients with stable angina and acute coronary syndromes. Polish National Registry. *Kardiol Pol.* 2014;72:1394-9.

6. Sabaté M, Windecker S, Iñiguez A, Okkels-Jensen L, Cequier A, Brugaletta S, Hofma SH, Räber L, Christiansen EH, Suttorp M, Pilgrim T, Anne van Es G, Sotomi Y, Garcia-Garcia HM, Onuma Y, Serruys PW. Everolimus-eluting bioresorbable stent vs. durable polymer everolimus-eluting metallic stent in patients with ST-segment elevation myocardial infarction: results of the randomized ABSORB ST-segment elevation myocardial infarction-TROFI II trial. *Eur Heart J.* 2016;37:229-40.

7. Kochman J, Tomaniak M, Kołtowski Ł, Jąkała J, Proniewska K, Legutko J, Roleder T, Pietrasik A, Rdzanek A, Kochman W, Brugaletta S, Kaluza GL. A 12-month angiographic and optical coherence tomography follow-up after bioresorbable vascular scaffold implantation in patients with ST-segment elevation myocardial infarction. *Catheter Cardiovasc Interv.* 2015;86:E180-9.

8. Task Force on the management of ST-segment elevation acute myocardial infarction of the European Society of Cardiology (ESC), Steg PG, James SK, Atar D, Badano LP, Blömstrom-Lundqvist C, Borger MA, Di Mario C, Dickstein K, Ducrocq G, Fernandez-Aviles F, Gershlick AH, Giannuzzi P, Halvorsen S, Huber K, Jüni P, Kastrati A, Knuuti J, Lenzen MJ, Mahaffey KW, Valgimigli M, van 't Hof A, Widimsky P, Zahger D. ESC Guidelines for the management of acute myocardial infarction in patients presenting with ST-segment elevation. *Eur Heart J.* 2012;33:2569-619.

9. Oberhauser JP, Hossainy S, Rapoza RJ. Design principles and performance of bioresorbable polymeric vascular scaffolds. *EuroIntervention.* 2009;5 Suppl F:F15-22.

10. Foin N, Gutiérrez-Chico JL, Nakatani S, Torii R, Bourantas CV, Sen S, Nijjer S, Petraco R, Kousera C, Ghione M, Onuma Y, Garcia-Garcia HM, Francis DP, Wong P, Di Mario C, Davies JE, Serruys PW. Incomplete stent apposition causes high shear flow disturbances and delay in neointimal coverage as a function of strut to wall detachment distance: implications for the management of incomplete stent apposition. *Circ Cardiovasc Interv.* 2014;7:180-9.

11. Cutlip DE, Windecker S, Mehran R, Boam A, Cohen DJ, van Es GA, Steg PG, Morel MA, Mauri L, Vranckx P, McFadden E, Lansky A, Hamon M, Krucoff MW, Serruys PW; Academic Research Consortium. Clinical end points in coronary stent trials: a case for standardized definitions. *Circulation.* 2007;115:2344-51.

12. Tuinenburg JC, Koning G, Hekking E, Zwinderman AH, Becker T, Simon R, Reiber JH. American College of Cardiology/European Society of Cardiology international study of angiographic data compression phase II. The effects of varying JPEG data compression levels on the quantitative assessment of the degree of stenosis in digital coronary angiography. *Eur Heart J.* 2000;21:679-86.

13. Onuma Y, Serruys PW, Muramatsu T, Nakatani S, van Geuns RJ, de Bruyne B, Dudek D, Christiansen E, Smits PC, Chevalier B, McClean D, Koolen J, Windecker S, Whitbourn R, Meredith I, Garcia-Garcia HM, Veldhof S, Rapoza R, Ormiston JA. Incidence and imaging outcomes of acute scaffold disruption and late structural discontinuity after implantation of the absorb Everolimus-Eluting fully bioresorbable vascular scaffold: optical coherence tomography assessment in the ABSORB cohort B Trial (A Clinical Evaluation of the Bioabsorbable Everolimus Eluting Coronary Stent System in the Treatment of Patients With De Novo Native Coronary Artery Lesions). *JACC Cardiovasc Interv.* 2014;7:1400-11.

14. Brugaletta S, Radu MD, Garcia-Garcia HM, Heo JH, Farooq V, Girasis C, van Geuns RJ, Thuesen L, McClean D, Chevalier B, Windecker S, Koolen J, Rapoza R, Miquel-Hebert K, Ormiston J, Serruys PW. Circumferential evaluation of the neointima by optical coherence tomography after ABSORB bioresorbable vascular scaffold implantation: can the scaffold cap the plaque? *Atherosclerosis.* 2012;221:106-12.

15. Gomez-Lara J, Radu M, Brugaletta S, Farooq V, Diletti R, Onuma Y, Windecker S, Thuesen L, McClean D, Koolen J, Whitbourn R, Dudek D, Smits PC, Regar E, Veldhof S, Rapoza R, Ormiston JA, Garcia-Garcia HM, Serruys PW. Serial analysis of the malapposed and uncovered struts of the new generation of everolimus-eluting bioresorbable scaffold with optical coherence tomography. *JACC Cardiovasc Interv.* 2011;4:992-1001.

16. Bourantas CV, Farooq V, Zhang Y, Muramatsu T, Gogas BD, Thuesen L, McClean D, Chevalier B, Windecker S, Koolen J, Ormiston J, Whitbourn R, Dorange C, Rapoza R, Onuma Y, Garcia-Garcia HM, Serruys PW. Circumferential distribution of the neointima at six-month and two-year follow-up after a bioresorbable vascular scaffold implantation: a substudy of the ABSORB Cohort B Clinical Trial. *EuroIntervention.* 2015;10:1299-306.

17. Ormiston JA, Serruys PW, Onuma Y, van Geuns RJ, de Bruyne B, Dudek D, Thuesen L, Smits PC, Chevalier B, McClean D, Koolen J, Windecker S, Whitbourn R, Meredith I, Dorange C, Veldhof S, Hebert KM, Rapoza R, Garcia-Garcia HM. First serial assessment at 6 months and 2 years of the second generation of absorb everolimus-eluting bioresorbable vascular scaffold: a multi-imaging modality study. *Circ Cardiovasc Interv.* 2012;5:620-32.

18. Serruys PW, Onuma Y, Garcia-Garcia HM, Muramatsu T, van Geuns RJ, de Bruyne B, Dudek D, Thuesen L, Smits PC, Chevalier B, McClean D, Koolen J, Windecker S, Whitbourn R, Meredith I, Dorange C, Veldhof S, Hebert KM, Rapoza R, Ormiston JA. Dynamics of vessel wall changes following the implantation of the absorb everolimus-eluting bioresorbable vascular scaffold: a multi-imaging modality study at 6, 12, 24 and 36 months. *EuroIntervention.* 2014;9:1271-84.

19. Park SJ, Kang SJ, Virmani R, Nakano M, Ueda Y. In-stent neoatherosclerosis: a final common pathway of late stent failure. *J Am Coll Cardiol.* 2012;59:2051-7.

20. Onuma Y, Sotomi Y, Shiomi H, Ozaki Y, Namiki A, Yasuda S, Ueno T, Ando K, Furuya J, Igarashi K, Kozuma K, Tanabe K, Kusano H, Rapoza R, Popma JJ, Stone GW, Simonton C, Serruys PW, Kimura T. Two-year clinical, angiographic, and serial optical coherence tomographic follow-up after implantation of an everolimus-eluting bioresorbable scaffold and an everolimus-eluting metallic stent: insights from the randomised ABSORB Japan trial. *EuroIntervention.* 2016;12:1090-101.

Supplementary data

Supplementary Appendix. OCT analysis methods.

Supplementary Table 1. Baseline clinical characteristics for the overall screened population of STEMI patients treated with primary PCI (n=132 patients) and patients with available two-year OCT data included in the present analysis (n=18 patients).

Supplementary Table 2. Baseline clinical characteristics (n=18 patients).

Supplementary Table 3. Serial optical coherence tomography analysis excluding the TLR patient (scaffold level, n=21).

Supplementary Table 4. OCT analysis - proximal, central and distal in-scaffold segment analysis.

Supplementary Table 5. Changes in lumen area of the adjacent peri-scaffold and in-scaffold subsegments.

Supplementary Figure 1. Study flow chart.

Supplementary Figure 2. Intra- and inter-observer variability for lumen area and scaffold area.

The supplementary data are published online at: http://www.pcronline.com/eurointervention/133rd_issue/362

Supplementary data

Supplementary Appendix. OCT analysis methods

Segment analysis, including in-scaffold and 5 mm adjacent peri-scaffold segments, was conducted at 1 mm longitudinal intervals. Additional analysis was performed for proximal, middle and distal segments defined as the three equal parts of the scaffold. The scaffold edge was defined as the first cross-section exhibiting visible struts in a circumference >270 degrees [15].

The neointimal area encompassed the new endothelial tissue as well as the strut core area and was defined as the difference between the scaffold area and the lumen area **(Figure 1)**. The neointimal thickness was measured at one-degree intervals [13-15]. The symmetry index of the neointima was calculated as the ratio of minimum/maximum neointimal thickness.

The malapposed struts were excluded from the neointimal area measurements as this may negatively impact on the measurements' reliability [14,16]. Nevertheless, the ratio of malapposed struts, recognised if there was any clear separation from the vessel wall, was quantified in relation to all struts analysed. In addition, the malapposition distance and area were calculated. Anatomical landmarks, such as calcifications and side branches were used to identify the corresponding baseline and follow-up OCT frames.

Strut discontinuity was recognised if two struts overhung each other in the same angular sector of the lumen perimeter or if they were isolated at the centre of the vessel without obvious connection with other surrounding struts [13]. In addition, the healing score (HS) was calculated at 12 and 24 months post procedure, according to the following formula: HS=[% ILDx4]+[% MUx3]+[% Ux2]+[% M], where the ILD stands for intraluminal defect, MU for malapposed and uncovered struts, U for uncovered struts, M for malapposed struts multiplied by respective weighting points [6]. Low HS reflects a favourable healing process without intraluminal defect, malapposition or uncovered struts, whereas a high HS indicates a poor healing pattern with thrombus, uncovered or malapposed struts [16].

Supplementary Table 1. Baseline clinical characteristics for the overall screened population of STEMI patients treated with primary PCI (n=132 patients) and patients with available two-year OCT data included in the present analysis (n=18 patients).

Patient characteristics	Overall STEMI population screened* (n=132)	STEMI patients treated with BVS included in the present analysis (n=18)	*p*-value
Age, years (mean±SD)	59.5±10.3	57.7±8.4	0.449
Male gender, n (%)	85 (64.4)	12 (66.7)	0.442
Diabetes, n (%)	14 (10.6)	2 (11.1)	0.786
Hypertension requiring medication, n (%)	103 (78.0)	14 (77.8)	0.654
Hyperlipidaemia requiring medication, n (%)	112 (84.8)	15 (83.3)	0.675
Current smoker, n (%)	80 (60.6)	12 (66.7)	0.198
COPD, n (%)	2 (1.5)	0 (0.0)	0.967
Prior myocardial infarction, n (%)	9 (6.8)	1 (5.6)	0.654
Prior CABG, n (%)	0 (0.0)	0 (0.0)	1.000
Peripheral vascular disease, n (%)	6 (4.5)	1 (5.6)	0.865
Kidney disease (eGFR <60 ml/min), n (%)	8 (6.1)	1 (5.6)	0.467

Data are expressed as mean±SD, median and IQR, or number (n) and percentage (%).
* refers to all STEMI patients treated with any type of stent implantation (BMS, DES, BVS).
CABG: coronary artery bypass graft; COPD: chronic obstructive pulmonary disease; eGFR: estimated glomerular filtration rate; IQR: interquartile range; SD: standard deviation

Supplementary Table 2. Baseline clinical characteristics (n=18 patients).

Patient characteristics	n=18
Age, years (mean±SD)	57.7±8.4
Male gender, n (%)	12 (66.7)
Diabetes, n (%)	2 (11.1)
Hypertension requiring medication, n (%)	14 (77.8)
Hyperlipidaemia requiring medication, n (%)	15 (83.3)
Current smoker, n (%)	12 (66.7)
COPD, n (%)	0 (0.0)
Prior myocardial infarction, n (%)	1 (5.6)
Prior CABG, n (%)	0 (0.0)
Peripheral vascular disease, n (%)	1 (5.6)
Kidney disease (eGFR <60 ml/min), n (%)	1 (5.6)

Data are expressed as mean±SD, median and IQR, or number (n) and percentage (%).

CABG: coronary artery bypass graft; COPD: chronic obstructive pulmonary disease; eGFR: estimated glomerular filtration rate; IQR: interquartile range; SD: standard deviation

Supplementary Table 3. Serial optical coherence tomography analysis excluding TLR patient (scaffold level, n=21).

Variable	Post procedure	12-month follow-up	24-month follow-up	Baseline-12 months	12-24 months	Baseline – 24 months	Baseline–12 months *p*-value	12–24 months *p*-value	Baseline–24 months *p*-value
Minimum lumen area (mm^2)	6.68±1.43	5.16±1.45	4.74±1.43	-1.61±0.94	-0.42±0.92	-2.08±1.08	<0.01	0.06	<0.01
Minimum flow area (mm^2)	6.59±1.44	5.16±1.45	4.74±1.43	-1.52±1.00	-0.42±0.93	-1.99±1.11	<0.01	0.06	<0.01
Mean lumen area (mm^2)	8.60±1.70	7.18±1.55	7.09±1.56	-1.55±0.92	-0.09±0.86	-1.61±1.21	<0.01	0.68	<0.01
Mean flow area (mm^2)	8.50±1.70	7.18±1.55	7.09±1.55	-1.45±0.91	-0.09±0.87	-1.52±1.20	<0.01	0.62	<0.01
Minimum scaffold area (mm^2)	7.02±1.51	7.33±1.33	7.41±1.62	0.25±1.01	0.07±0.86	0.26 ±0.93	0.23	0.69	0.25
Mean scaffold area (mm^2)	8.38±1.59	9.09±1.47	9.95±1.71	0.25±1.01	0.07±0.86	0.26±0.93	<0.01	<0.01	<0.01
Scaffold-to-vessel diameter ratio	1.00±0.00	1.14±0.05	1.20±0.06	0.14±0.05	0.06±0.04	0.20±0.06	<0.01	<0.01	<0.01
Scaffold area obstruction (%)	0.00±0.00	21.60±6.67	29.27±6.71	21.60±6.67	7.66±4.73	29.27±6.71	<0.01	<0.01	<0.01
Distal reference mean lumen area (mm^2)	7.02±3.46	7.18±2.86	6.95±2.71	0.08±2.21	-0.43±1.06	-0.40±1.93	0.31	0.04	0.68
Proximal reference mean lumen area (mm^2)	8.76±3.29	8.40±3.14	8.37±3.09	-1.40±2.10	-0.14±1.05	-1.24±2.49	0.04	0.67	0.17
Malapposed strut ratio (%)*	5.2±8.6	0.3±1.5	0.2±1.1	-4.9±7.2	-0.1±0.4	-5.0±7.6	<0.01	0.33	0.01
Malapposed strut ratio (%) in patients with any malapposed strut*	7.2±9.5 (n=13)	6.6±0.0 (n=1)	4.7±0.0 (n=1)	-0.6±0.0	-1.8±0.0	-2.5±0.0	-	-	-
Malapposition distance (mm)*	0.12±0.09	0.03±0.12	0.02±0.09	-0.09±0.11	-0.01±0.03	-0.09±0.09	<0.01	0.33	<0.01
Malapposition area (mm^2)*	0.34±0.50	0.07±0.31	0.05±0.22	-0.26±0.39	-0.02±0.10	-0.28±0.40	0.01	0.33	0.01
Mean neointima thickness (µm)	0±0	204±43	272±48	204±43	67±35	272±48	<0.01	<0.01	<0.01
Maximum neointimal thickness (µm)	0±0	346±45	437±68	346±45	80±56	437±68	<0.01	0.01	<0.01
Neointima area (mm^2)	0.00±0.00	1.91±0.50	2.86±0.66	1.91±0.50	0.95±0.50	2.86±0.66	<0.01	<0.01	<0.01
Symmetry of the neointima thickness	-	0.85±0.13	0.71±0.13	-	-0.13±0.10	-	-	<0.01	-
Uncovered strut ratio (%)	-	1.1±1.8	0.4±1.2	-	-0.6±2.2	-	-	0.24	-
Uncovered strut ratio (%) in patients with any uncovered struts	-	2.5±2.0	1.7±2.1	-	-0.4±5.0	-	-	0.57	-
Scaffolds with > 0 uncovered struts, n (%)	-	8 (42.1)	5 (26.3)	-	3	-	-	0.26	-
Scaffolds with >0 malapposed struts, n (%)	13 (72.2)	1 (5.3)	1 (5.3)	12	0	12	<0.01	1.00	<0.01
Healing score	-	2.46±4.70	1.15±2.84	-	1.31±4.59	-	-	0.16	-

Data expressed as mean and standard deviation or count and percentage (%).

* Malapposition at baseline was found in 13 patients; at 12 and 24 months malapposition was present in 1 patient.

Supplementary Table 4. Optical coherence tomography analysis – proximal, central and distal in-scaffold segment analysis.

Variable	Proximal in-scaffold segment	Middle in-scaffold segment	Distal in-scaffold segment
Mean lumen area (mm^2)			
Post-procedure (n=19)	8.98±1.97	7.71±1.57	8.45±2.12
12-month (n=20)	7.33±2.05	6.78±1.64	6.76±1.91
24-month (n=20)	7.34±2.24	7.21±1.78	6.47±1.94
p-value baseline-12 mo	<0.01	<0.01	<0.01
p-value 12 mo-24 mo	0.95	0.05	0.31
p-value baseline-24 mo	<0.01	0.10	<0.01
Mean scaffold area (mm^2)			
Post-procedure	8.52±1.56	8.11±1.56	8.37±1.81
12-month	9.45±1.89	8.91±1.54	8.61±1.63
24-month	10.33±2.31	10.07±1.88	9.19±2.10
p-value baseline-12 mo	0.02	<0.01	0.44
p-value 12 mo-24 mo	0.01	<0.01	0.02
p-value baseline-24 mo	0.01	<0.01	0.01
Malapposition area (mm^2)			
Post-procedure	0.38±0.83	0.06±0.15	0.11±0.13
12-month	0.07±0.32	0.05±0.21	0.00±0.00
24-month	0.05±0.22	0.04±0.18	0.00±0.00
p-value baseline-12 mo	<0.01	0.88	<0.01
p-value 12 mo-24 mo	0.15	0.99	1.00
p-value baseline-24 mo	<0.01	0.74	<0.01
Malapposed strut total (n)			
Post-procedure	101	39	33
12-month	14	2	Lack of malapposition
24-month	9	2	Lack of malapposition
Malapposition distance (mm)			
Post-procedure	0.09±0.12	0.04±0.07	0.06±0.07
12-month	0.03±0.12	0.03±0.13	0.00±0.00
24-month	0.02±0.08	0.03±0.12	0.00±0.00
p-value baseline-12 mo	<0.01	0.55	<0.01
p-value 12 mo-24 mo	0.30	0.65	1.00
p-value baseline-24 mo	<0.01	0.33	<0.01
Mean neointima thickness (µm)			
Post-procedure	0.0±0.0	0.0±0.0	0.0±0.0
12-month	223±82	224±68	206±82
24-month	282±83	285±57	270±56
p-value baseline-12 mo	<0.01	<0.01	<0.01
p-value 12 mo-24 mo	<0.01	<0.01	<0.01
p-value baseline-24 mo	<0.01	<0.01	<0.01
Neointima area (mm^2)			
Post-procedure	0.00±0.00	0.00±0.00	0.00±0.00
12-month	2.12±0.66	2.13±0.52	1.85±0.74
24-month	2.99±1.11	2.86±0.53	2.71±0.74
p-value baseline-12 mo	<0.01	<0.01	<0.01
p-value 12 mo-24 mo	<0.01	<0.01	<0.01
p-value baseline-24 mo	<0.01	<0.01	<0.01
Uncovered strut ratio (%)			
Post-procedure	-	-	-
12-month	0.9±2.3	0.6±1.3	1.4±3.5
24-month	0.9±3.3	0.1±0.4	0.3±0.7
p-value baseline-12 mo	-	-	-
p-value 12 mo-24 mo	0.95	0.17	0.20
p-value baseline-24 mo	-	-	-

Uncovered strut ratio in patients with any uncovered struts (%)			
Post-procedure	-	-	-
12-month	4.7±3.3 (n=4)	2.8±1.7 (n=4)	9.1±3.1 (n=3)
24-month	5.9±7.7 (n=1)	2.0±0.0 (n=1)	1.9±0.7 (n=1)
p-value baseline-12 mo	-	-	-
p-value 12 mo-24 mo	1.00	-	1.00
p-value baseline-24 mo	-	-	-

Data expressed as mean and standard deviation or count and percentage (%),
p-value – paired Wilcoxon test.

Supplementary Table 5. Changes in lumen area of the adjacent peri-scaffold and in-scaffold subsegments.

Variable	Proximal edge	Proximal segment	Middle segment	Distal segment	Distal edge
Mean lumen area (mm^2)					
Baseline–12 months	-1.31 (2.04)	-1.88 (1.40)	-1.02 (1.12)	-1.75 (1.18)	-0.7 (1.85)
12–24 months	0.01 (1.23)	0.01 (1.64)	0.43 (1.08)	-0.29 (0.90)	-0.29 (1.01)
Baseline–24 months	-1.23 (2.10)	-1.78 (1.75)	-0.59 (1.39)	-2.06 (1.22)	-0.95 (1.72)
p-value (baseline vs. 12 months)	0.0046	<0.0001	0.0010	<0.0001	0.1958
p-value (12 vs. 24 months)	0.9217	0.9530	0.1042	0.3124	0.1657
p-value (baseline vs. 24 months)	0.0323	0.0006	0.0546	<0.0001	0.0323
p-value P*	0.1688		*p*-value D*	0.0039	
p-value P**	0.9530		*p*-value D**	0.7680	
p-value P***	0.1688		*p*-value D***	0.0006	

p-value P* for the delta baseline vs. 12 months between the proximal edge and proximal segment.
p-value P** (12 months vs. 24 months).
p-value P*** (baseline vs. 24 months).

p-value D* for the delta baseline vs. 12 months between the distal edge and distal segment.
p-value D** (12 months vs. 24 months).
p-value D*** (baseline vs. 24 months).
D: between the distal edge and distal segment; P: between the proximal edge and proximal segment

Supplementary Figure 1. Study flow chart.

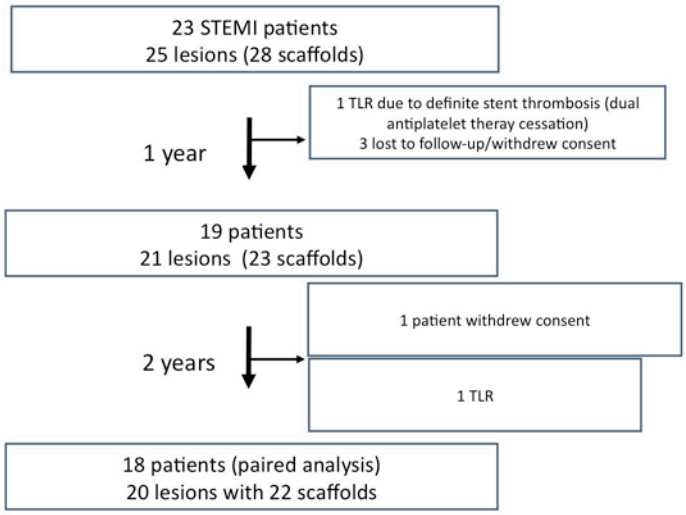

Supplementary Figure 2. Intra- and inter-observer variability for lumen area and scaffold area.